1776 *J. Am. Chem. Soc.* **2000,** *122,* 1776−1788

Ab Initio MO Study of the Global Potential Energy Surface of C_4H_4 in Triplet Electronic State and the Reactions of $C(^3P_j)$ with C_3H_4 (Allene and Propyne) and $C_2(A^3\Pi_u)$ with $C_2H_4(X^1A_{1g}{}^+)$

A. M. Mebel,*[†,‡] R. I. Kaiser,[†,§,||] and Y. T. Lee[†]

Contribution from the Institute of Atomic and Molecular Sciences, Academia Sinica, P.O. Box 23-166, Taipei 10764, Taiwan, Department of Chemistry, Tamkang University, Tamsui 25137, Taiwan, Department of Physics, Technical University Chemnitz-Zwickau, 09107 Chemnitz, Germany, and Department of Physics, National Taiwan University, Taipei 106, Taiwan

Received October 1, 1999. Revised Manuscript Received December 14, 1999

Abstract: The global potential energy surface of C_4H_4 in the lowest triplet electronic state have been studied at the G2M(RCC,MP2) level. Of 28 distinct isomers the most stable are aromatic cyclobutene **q3** ($^3A_{1g}$,D_{4h}) and linear butyne **c1** (^3E,D_{2d}), and 66 transition states for various isomerization and dissociation pathways have been found. The information about the global PES is applied to describe the potential energy surfaces for the $C(^3P_j) + H_2CCCH_2$, $C(^3P_j) + H_3CCCH$, and $C_2(^3\Pi_u) + C_2H_4$ reactions, recently studied experimentally in crossed molecular beams. The reaction of the carbon atom with allene is shown to occur by a barrierless addition of C to the C═C bond to yield the three-member ring structure **t1** and/or to the central carbon atom of allene to form the branching structure **b1** which isomerizes to **t1** with a low barrier. **t1** undergoes ring opening to **c1** with a barrier of 9.4 kcal/mol, and the latter emits a H atom to give the major reaction product *n*-C_4H_3 with an exit barrier of 2.2 kcal/mol. The minor reaction product, *i*-C_4H_3, is formed through a 1,2-H shift in **c1** leading to **c3**, followed by the hydrogen loss. The reaction of the carbon atom with methylacetylene starts with a barrierless C addition to the β-C-atom of H_3CCCH to form **c6**, to the α-C-atom to give **b2** or **b2′**, or to the acetylenic C≡C bond to yield the cyclic isomers **t4** or **t4′**. **c6**, **b2**, and **b2′** are metastable and would rapidly rearrange to the linear isomer **c5** or to the cyclic **t4** and then to **t4′** with low barriers. The latter ring opens to **c5** with a barrier of 14.7 kcal/mol. At high collision energies, the major reaction product *n*-C_4H_3 is formed through the methyl hydrogen emission in **c5** with an exit barrier of 5.8 kcal/mol. The second product *i*-C_4H_3 can be reached via a H-shift from **c5** to **c4** and subsequent hydrogen elimination. Cyclic isomers C_4H_3 **p3** and **p4** can originate from **t4**, **t4′**, and **t5**. The reaction of $C_2(^3\Pi_u)$ with ethylene proceeds through a C_2 addition to a carbon atom of C_2H_4 to yield the chain isomer **c2** with an entrance barrier of ∼4 kcal/mol. **c2** rearranges to linear **c1** in several steps via the four-member ring intermediate **q1** or the three-membered ring structures **t2** and **t1**. **c1** loses a H atom to yield *n*-C_4H_3 or undergoes a hydrogen migration to **c3** followed by a H emission producing *n*- or *i*-C_4H_3. Similarly to $C(^3P_j)$ + allene, *n*-C_4H_3 is expected to be the major product of $C_2(^3\Pi_u) + C_2H_4$, while *i*-C_4H_3 to give a minor contribution.

Introduction

Formation of various structural isomers of hydrocarbon radicals and their chemical reactivity is relevant to chemical processes in hydrocarbon-rich planetary atmospheres,[1] outflow of dying carbon stars, interstellar clouds, and hot molecular cores.[2] The reactivity of such radicals is also of major importance in combustion chemistry.[3] Take, for instance, C_4H_3. In oxygen-deficient combustion, *n*- and *i*-C_4H_3 isomers are believed to play a crucial role in formation of the first aromatic ring, the phenyl radical C_6H_5, via the reaction with acetylene.[4] On the other hand, cyclic isomers are expected not to form aromatic species. The distinct isomers of C_4H_3 can be produced in the carbon−hydrogen exchange channel in the reactions of atomic carbon $C(^3P_j)$ with two structural isomers of C_3H_4, allene CH_2CCH_2, and methylacetylene (propyne) CH_3CCH, as was recently demonstrated by crossed molecular-beam experiments.[5,6] Similar carbon−hydrogen exchange reactions occur when $C(^3P_j)$ attacks acetylene (the products are l/c−C_3H + H), ethylene (producing C_3H_3 + H), C_3H_6 (producing C_4H_5 + H), C_3H_3 (producing C_4H_2 + H), and C_6H_6 (producing C_7H_5 + H).[7] The molecular-beam measurements carried out in the single collision conditions support the hypothesis that C_4H_3 isomers are likely to be formed in such extraterrestrial environments as cold molecular clouds and planetary atmospheres of Jupiter, Saturn, Uranus, and Neptune as well as the moons Titan and Triton.[5,6]

[†] Academia Sinica.

[‡] Tamkang University.

[§] Technical University Chemnitz-Zwickau.

[||] National Taiwan University.

(1) Proceedings of the Symposium on Titan. ESA Special publication 338; ESTEC: Noordwijk, Netherlands, 1992.

(2) Herbst, E.; Lee, H. H.; Howe, D. A.; Millar, T. *Mon. Not. R. Astron. Soc.* **1994**, *268*, 335.

(3) (a) Kern, R. D.; Xie, K.; Chen, H. *Combust. Sci. Technol.* **1992**, *85*, 77. (b) Smith, R. D. *Combust. Flame* **1979**, *35*, 179. (c) Slagle, I. R.; Gutman, D. *Proc. 23rd Symp. Int. Combust. Chem.* **1988**, 875. (d) Thorne, L. R.; Branch, M. C.; Chandler, D. W.; Kee, R. J.; Miller, J. *Proc. 21st Symp. Int. Combust. Chem.* **1986**, 965.

(4) (a) Westmoreland, P. R. et al. *J. Phys. Chem.* **1989**, *93*, 8171. (b) Walsh, S. P.; *J. Chem. Phys.* **1995**, *103*, 8544. (c) Madden, L. K.; Moskaleva, L. V.; Kristyan, S.; Lin, M. C. *J. Phys. Chem. A* **1997**, *101*, 6790.

(5) Kaiser, R. I.; Stranges, D.; Lee, Y. T.; Suits, A. G. *J. Chem. Phys.* **1996**, *105*, 8721.

(6) Kaiser, R. I.; Mebel, A. M.; Chang, A. H. H.; Lin, S. H.; Lee, Y. T. *J. Chem. Phys.* **1999**, *110*, 10330.

10.1021/ja9935299 CCC: $19.00

The use of the crossed molecular-beam technique allows us to elucidate the intimate chemical dynamics of the neutral reaction of atomic carbon $C(^3P_j)$ or carbon dimer C_2 with unsaturated hydrocarbons, to gain information at the center-of-mass angular flux and translational energy distributions of the reaction products and to derive energy-dependent triply differential cross-sections. On the other hand, chemically accurate (within 0.1 eV) ab initio molecular orbital (MO) calculations of potential energy surfaces (PES) for these reactions can serve as a complimentary approach which gives a deeper insight into the reaction mechanism and allows us to surmise the most important reaction channels and to predict branching ratios of various products based on RRKM calculations of reaction rate constants. Recently, experimental measurements were performed for the reactions $C(^3P_j) + CH_2CCH_2$,[6] $C(^3P_j) + CH_3CCH$,[5] and $C_2(^3\Pi_u) + C_2H_4$.[8] All three reactions explore different regions of the triplet PES for the C_4H_4 system. Our goal in the present paper is to investigate the global PES for triplet C_4H_4, i.e., to find all (or almost all) possible isomers of this species, to examine isomerization pathways connecting the local minima, and to study various dissociation channels. After that, we can closely analyze the potential energy surfaces for the reaction of atomic carbon with allene and propyne and C_2 with ethylene.

Computational Methods

The geometries of various isomers of triplet C_4H_4, transition states for isomerization and dissociation, as well as dissociation products, have been optimized using the hybrid density functional B3LYP method,[9] with the 6-311G(d,p) basis set.[10] Vibrational frequencies, calculated at the B3LYP/6-311G(d,p) level, have been used for characterization of stationary points and zero-point energy (ZPE) correction without scaling. All the stationary points have been positively identified for minimum (number of imaginary frequencies NIMAG=0) or transition state (NIMAG=1). All the energies quoted and discussed in the present paper include the ZPE correction. In some cases mentioned in Discussion, geometries and frequencies were also calculated at the MP2/6-311G(d,p)[11] and CCSD(T)/6-311G(d,p)[12] levels.

To obtain more reliable energies of the most important equilibrium structures and transition states, we used the G2M(RCC,MP2) method,[13] which gives an approximation to the RCCSD(T)/6-311+G(3df,2p)[12] energy. It is known that the expected accuracy of this and other G2-type calculational schemes is within 1−2 kcal/mol.[13−16] The GAUSSIAN 94,[17] MOLPRO 96,[18] and ACES−II[19] programs were employed for the calculations.

Results and Discussion

Isomers of Triplet C_4H_4. To survey various possible isomers of triplet C_4H_4, we consider different arrangements of four carbon atoms and different distributions of four hydrogens between them. Four C atoms can form a chain, a branch with the central carbon with three CC bonds, a three-membered ring with an out-of-ring CC bond, a four-membered ring, and a bicyclic structure where two three-membered rings are fused together. Figure 1 shows optimized structures of various isomers. In this figure, chain isomers are denoted with the letter "c", branching structures with "b", three-member rings with "t", and four-member rings and bicyclic structures with "q".

The largest number of isomers, 13, is found for the chain arrangement. The most stable of them is H_2CCCCH_2 **c1**. It has a linear geometry with D_{2d} symmetry and ^3E electronic state. **c1** can be described as a triplet butyne with the central triple $C{\equiv}C$ bond, two single $C{-}C$ bonds, and two radical centers (unpaired electrons) on the terminal carbons. However, the triple bond, 1.25 Å, is longer than the regular triple bond (1.20 Å in acetylene)[20] and the single bonds are much shorter than regular single bonds. This indicates a presence of some contributions from the $H_2C{=}C{=}C^{\bullet}{-}C^{\bullet}H_2$ and $H_2C^{\bullet}{-}C^{\bullet}{=}C{=}CH_2$ resonance structures in the wave function of **c1**. At the G2M(RCC,MP2) level **c1** lies 41.1 kcal/mol higher in energy than singlet butatriene $H_2C{=}C{=}C{=}CH_2$. The next in the order of stability chain isomer is **c5**, H_3CCCCH, which is 6.9 kcal/mol less favorable than **c1**. In terms of resonance structures, **c5** can be described as a mixture of $H_3C{-}C{\equiv}C{-}C^{\bullet\bullet}H$ and $H_3C{-}C^{\bullet}{=}C{=}C^{\bullet}H$. Apparently, the latter has a larger contribution since two CC bonds have similar bond lengths of 1.26 and 1.28 Å. **c5** has no symmetry, and the geometry is substantially nonlinear, with the CCH angle of 160°, but two CCC angles are close to 180°. Next two isomers **c4** ($H_2C^{\bullet}{-}C^{\bullet}H{-}C{\equiv}CH$) and **c3** ($H_2C{=}C{=}CH{-}C^{\bullet\bullet}H \leftrightarrow H_2C{=}C^{\bullet}{-}CH{=}C^{\bullet}H$) have C_s symmetry and $^3A''$ electronic state and lie, respectively, 13.2 and 20.1 kcal/mol higher in energy than **c1**.

Three configurations are about 32−33 kcal/mol less stable than **c1**. **c10**, $HC{\equiv}C{-}CH_2{-}C^{\bullet\bullet}H$, is C_s-symmetric, has a $^3A''$ electronic state and exhibits a typical carbene structure with the CCH angle of 133° (ca. with 136° for HCH in triplet CH_2).[20] **c9** and **c9′** are different conformers of $HC^{\bullet}{=}CH{-}CH{=}C^{\bullet}H$.

---

(7) (a) Ochsenfeld, C.; Kaiser, R. I.; Suits, A. G.; Lee, Y. T.; Head-Gordon, M. *J. Chem. Phys.* **1997**, *106*, 4141. (b) Kaiser, R. I.; Ochsenfeld, C.; Head-Gordon, M.; Lee, Y. T.; Suits, A. G. *Science* **1996**, 274, 1508. (c) Kaiser, R. I.; Lee, Y. T.; Suits, A. G. *J. Chem. Phys.* **1996**, *105*, 8705. (d) Kaiser, R. I.; Stranges, D.; Bevsek, H. M.; Lee, Y. T.; Suits, A. G. *J. Chem. Phys.* **1997**, *106*, 4945. (e) Kaiser, R. I.; Sun, W.; Suits, A. G.; Lee, Y. T. *J. Chem. Phys.* **1997**, *107*, 8713. (f) Kaiser, R. I.; Hahndorf, I.; Huang, L. C. L.; Lee, Y. T.; Bettinger, H. F.; Schleyer, P. v. R.; Schaefer, H. F., III; Schreiner, P. R. *J. Chem. Phys.* **1999**, *110*, 6091.

(8) Balucani, N.; Asvany, O.; Mebel, A. M.; Lee, Y. T.; Kaiser, R. I., to be published.

(9) (a) Becke, A. D. *J. Chem. Phys.* **1993**, *98*, 5648. (b) *Ibid.* **1992**, *96*, 2155. (c) *ibid.* **1992**, *97*, 9173; Lee, C.; Yang, W.; Parr, R. G. *Phys. Rev.* **1988**, *B 37*, 785.

(10) Krishnan, R.; Frisch, M.; Pople, J. A. *J. Chem. Phys.* **1980**, *72*, 4244.

(11) Hehre, W. J.; Radom, L.; Schleyer, P. v. R.; Pople, J. *Ab Initio Molecular Orbital Theory*; Wiley: New York, 1986.

(12) (a) Purvis, G. D.; Bartlett, R. J. *J. Chem. Phys.* **1982**, *76*, 1910. (b) Hampel, C.; Peterson, K. A.; Werner, H.-J. *Chem. Phys. Lett.* **1992**, *190*, 1. (c) Knowles, P. J.; Hampel, C.; Werner, H.-J. *J. Chem. Phys.* **1994**, *99*, 5219. (d) Deegan, M. J. O.; Knowles, P. J. *Chem. Phys. Lett.* **1994**, *227*, 321.

(13) Mebel, A. M.; Morokuma, K.; Lin, M. C. *J. Chem. Phys.* **1995**, *103*, 7414.

(14) (a) Curtiss, L. A.; Raghavachari, K.; Trucks, G. W.; Pople, J. A. *J. Chem. Phys.* **1991**, *94*, 7221. (b) Pople, J. A.; Head-Gordon, M.; Fox, D. J.; Raghavachari, K.; Curtiss, L. A. *J. Chem. Phys.* **1989**, *90*, 5622. (c) Curtiss, L. A.; Jones, C.; Trucks, G. W.; Raghavachari, K.; Pople, J. A. *J. Chem. Phys.* **1990**, *93*, 2537.

(15) (a) Curtiss, L. A.; Raghavachari, K.; Pople, J. A. *J. Chem. Phys.* **1993**, *98*, 1293. (b) Smith, B. J.; Radom, L. *J. Phys. Chem.* **1995**, *99*, 6468. (c) Curtiss, L. A.; Redfern, P. C.; Smith, B. J.; Radom, L. *J. Chem. Phys.* **1996**, *104*, 5148.

(16) (a) Curtiss, L. A.; Raghavachari, K.; Redfern, P. C.; Pople, J. A. *J. Chem. Phys.* **1997**, *106*, 1063. (b) Curtiss, L. A.; Redfern, P. C.; Raghavachari, K.; Pople, J. A. *J. Chem. Phys.* **1998**, *109*, 42.

(17) Frisch, M. J.; Trucks, G. W.; Schlegel, H. B.; Gill, P. M. W.; Johnson, B. G.; Robb, M. A.; Cheeseman, J. R.; Keith, T.; Petersson, G. A.; Montgomery, J. A.; Raghavachari, K.; Al-Laham, M. A.; Zakrzewski, V. G.; Ortiz, J. V.; Foresman, J. B.; Cioslowski, J.; Stefanov, B. B.; Nanayakkara, A.; Challacombe, M.; Peng, C. Y.; Ayala, P. Y.; Chen, W.; Wong, M. W.; Andres, J. L.; Replogle, E. S.; Gomperts, R.; Martin, R. L.; Fox, D. J.; Binkley, J. S.; Defrees, D. J.; Baker, J.; Stewart, J. P.; Head-Gordon, M.; Gonzalez, C.; Pople, J. A. GAUSSIAN 94, Revision E.2; Gaussian, Inc.: Pittsburgh, PA, 1995.

(18) MOLPRO is a package of ab initio programs written by H.-J. Werner and P. J. Knowles, with contributions from J. Almlöf, R. D. Amos, M. J. O. Deegan, S. T. Elbert, C. Hampel, W. Meyer, K. Peterson, R. Pitzer, A. J. Stone, P. R. Taylor, and R. Lindh.

(19) Stanton, J. F.; Gauss, J.; Watts, J. D.; Lauderdale, W. J.; Bartlett, R. J. ACES-II, University of Florida, Gainesville, FL.

(20) *CRC Handbook of Chemistry and Physics*, 74 ed.; Lide, D. R., Ed.; Chemical Rubber: Boca Raton, 1993.

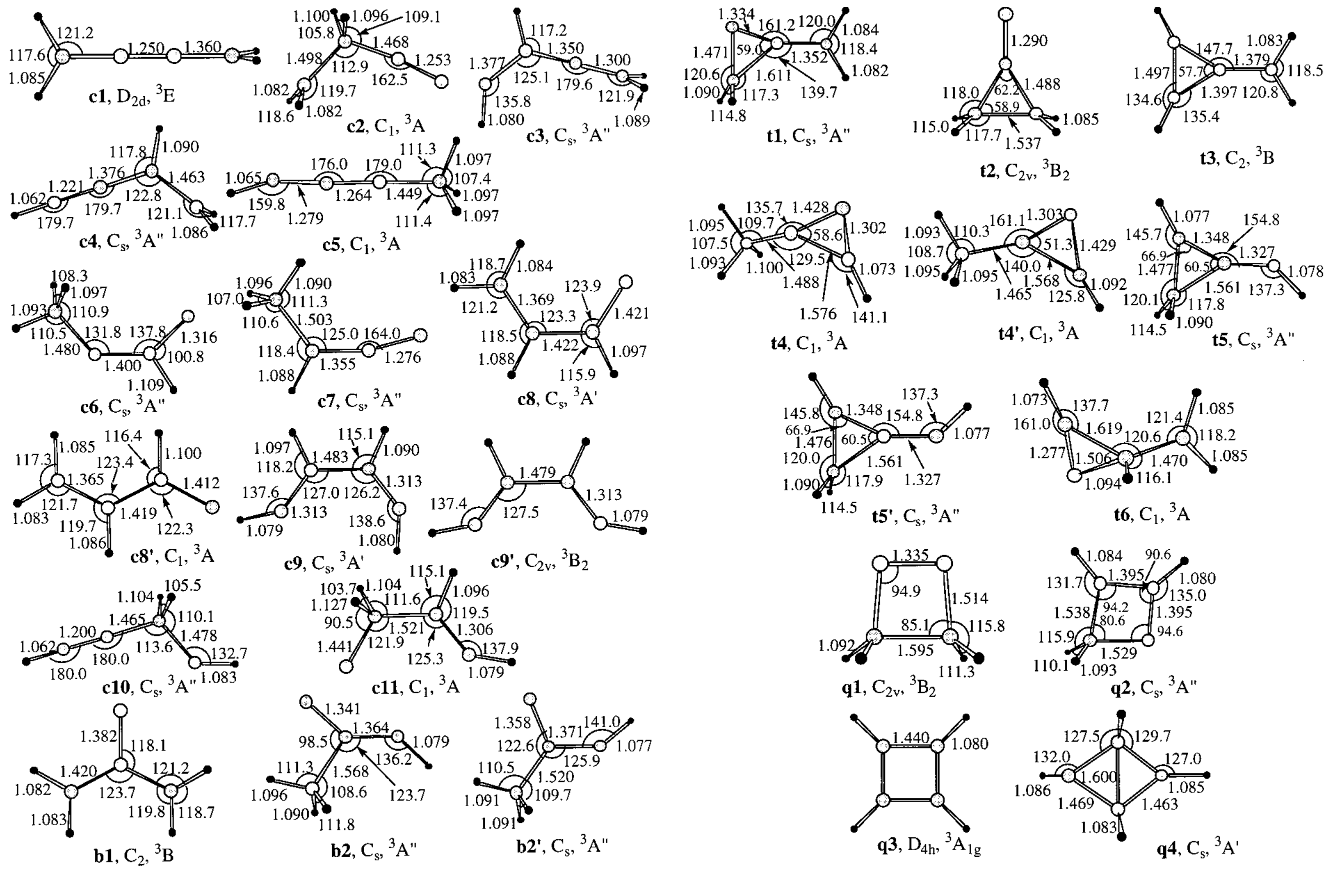

Figure 1. Optimized geometries (bond lengths are in Å, bond angles are in degrees) of various local minima for triplet C_4H_4.

c9′ ($^3B_2$,C_{2v}) is 0.3 kcal/mol more favorable than **c9** ($^3A'$,C_s). Interestingly, the **c9** → **c9′** isomerization occurs by the hydrogen in-plane scrambling rather than by rotation around the double C═C bond, and the barrier is relatively low, about 4 kcal/mol. More different conformers of triplet CHCHCHCH may exist, but we do not consider them here since they are expected to have similar energies with **c9** and **c9′** and are not relevant for the title reactions.

c7 ($^3A''$,C_s) lies 42.7 kcal/mol higher than **c1**. Its electronic structure can be described as a resonance of $H_3C{-}CH{=}C{=}C^{\bullet\bullet}$ and $H_3C{-}C^{\bullet}H{-}C{\equiv}C^{\bullet}$. **c8** and **c8′** correspond to two different conformers of triplet vinylvinylidene CH_2CHCHC. **c8** has a planar geometry and $^3A'$ electronic state, while **c8′** (^3A) slightly deviates from planarity. **c8** and **c8′** are similar in energy (the latter is about 1 kcal/mol more stable) and lie ~52 kcal/mol above **c1**. Although the most reasonable valence configuration for **c8** and **c8′** is $H_2C{=}CH{-}CH{=}C^{\bullet\bullet}$, alone it cannot explain the geometric structure where the central CH−CH and the terminal CH═C bonds have very close bond lengths of ~1.42 Å and the $H_2C{=}CH$ bond, 1.37 Å, is only slightly shorter. To rationalize this structure one can invoke two other possible resonance configurations: $H_2C^{\bullet}{-}CH{=}CH{-}C^{\bullet\bullet\bullet}$ and $H_2C^{\bullet}{-}C^{\bullet}H{-}CH{=}C^{\bullet\bullet}$. Lineberger and co-workers[21] assigned some peaks in the photoelectron spectrum of $C_4H_4^-$ to the triplet vinylvinylidene in the $^3A'$ electronic state. On the basis of the spectrum, they derived four vibrational frequencies for this state, at 360, 500, 835, and 1250 cm^{-1}. The closest to these values theoretical frequencies calculated at the B3LYP/6-311G(d,p) level and scaled by 0.9614 are 291, 532, 908, and 1260 cm^{-1} for **c8′** and 279, 504, 924, and 1240 cm^{-1} for **c8**. The agreement with experiment is worse than usually expected from the scaled B3LYP frequencies. Therefore, the assignment of the photoelectron spectrum of $C_4H_4^-$ may not be completely accurate.

c2 and **c6** are ~63 kcal/mol less stable than the isomer **c1**. **c2** has no symmetry, and its structure can be described as $H_2C^{\bullet}{-}CH_2{-}C{\equiv}C^{\bullet}$. Isomer **c6**, $H_3C{-}C^{\bullet\bullet}{-}CH{=}C^{\bullet\bullet}$, with possible small contribution from $H_3C{-}C^{\bullet}{=}CH{-}C^{\bullet\bullet\bullet}$ making the central CC bond shorter, is C_s-symmetric with $^3A''$ electronic state. The least stable isomer among the chain structures is **c11**, $C^{\bullet\bullet\bullet}{-}CH_2{-}CH{=}C^{\bullet}H$, which lies 85.6 kcal/mol higher in energy than **c1**. As will be seen in subsequent sections, **c11** dissociates to singlet acetylene and triplet vinylidene with a barrier of only 0.1 kcal/mol.

Three distinct branching isomers are found. **b1** is the most stable of them, 50.6 kcal/mol higher in energy than **c1**. The geometry of **b1** is C_2-symmetric, with ^3B electronic state. The electronic configuration can be expressed in terms of three resonance structures, $H_2C^{\bullet}{-}C({=}C^{\bullet\bullet}){-}C^{\bullet}H_2$, $H_2C{=}C({-}C^{\bullet\bullet\bullet}){-}C^{\bullet}H_2$, and $H_2C^{\bullet}{-}C({-}C^{\bullet\bullet\bullet}){=}CH_2$. This makes all three CC distances close to each other, 1.42 Å for $C{-}CH_2$ and 1.38 Å for $C{-}C^{\bullet\bullet}$. **b2** and **b2′** correspond to cis and trans conformers of $H_3CC(C)CH$. They are 17.7 and 15.7 kcal/mol less stable than **b1**. Both structures have C_s symmetry, $^3A''$ electronic state and $H_3C{-}C({=}C^{\bullet\bullet}){-}C^{\bullet\bullet}H \leftrightarrow H_3C{-}C({-}C^{\bullet\bullet\bullet}){=}C^{\bullet}H$ electronic configuration.

Most of eight three-membered ring isomers are more stable than the branching structures. For instance, **t1**, **t3**, **t5**, and **t5′** lie 32−34 kcal/mol above **c1**. **t1** ($^3A''$,C_s) has the electronic configuration described by the

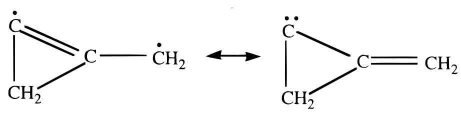

---

(21) Gunion, R. F.; Köppel, H.; Leach, G. W.; Lineberger, W. C, *J. Chem. Phys.* **1995**, *103*, 1250.

resonance. The electronic structure of C_2-symmetric **t3** in the ^3B state can be expressed as a mixture of

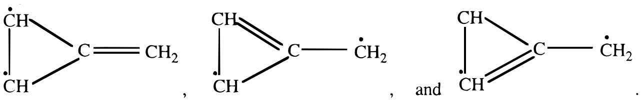

Thus, the double bond is delocalized between the carbon−carbon bonds with the bond lengths of 1.38−1.40 Å. **t5** and **t5′** are two conformers of

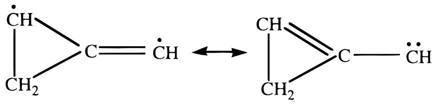

and both have C_s symmetry and $^3A''$ electronic state. Nonsymmetric structures **t4** and **t4′** are 45.3 and 43.3 kcal/mol less stable than **c1**, respectively. Their geometries and electronic structures are quite similar and differ only by the position of the ring double bond. One can express the structure of **t4** and **t4′** as

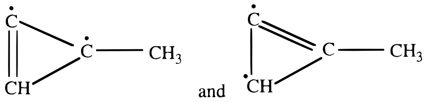

According to this bond arrangement, **t4** has the CH_3 group deviating out of the ring plane, while in **t4′** the CH hydrogen is out-of-plane and the methyl carbon is in-plane. **t4** and **t4′** have similar energies and rearrange to each other with a small barrier of 3.3 kcal/mol with respect to more stable **t4′**. In the corresponding transition state t4-t4′ the two bonds, C−C(H) and C−C(CH_3), exchanging the double bond character have similar lengths of 1.34−1.37 Å. By the energetic order, the next three membered ring isomer is **t6**, 50.6 kcal/mol less stable than **c1**. **t6** does not have any symmetry and its structure is described as

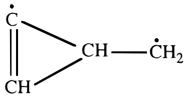

Finally, **t2** is the least stable three-member ring isomer lying 63.4 kcal/mol above **c1**. The structure of **t2** ($^3B_2$) is C_{2v}-symmetric and the electronic configuration is

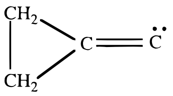

The last interesting group of triplet C_4H_4 isomers is represented by four-membered ring and bicyclic structures. Within this group we find the most stable configuration of triplet C_4H_4, **q3**, which lies 0.4 kcal/mol below the chain isomer **c1**. **q3**, triplet cyclobutene, is a structural analogue of singlet cyclobutadiene. The latter is well established to be a highly antiaromatic system.[22] On the contrary, triplet ($^3A_{1g}$) cyclobutene is aromatic according to its symmetric D_{4h} geometry. All four CC bonds in the cycle have the same length of 1.44 Å. Therefore, the only double bond in **q3** is delocalized among four carbon−carbon bonds and two unpaired electrons are also delocalized on all C atoms. Despite of its aromaticity, triplet cyclobutene lies ∼7.0 kcal/mol higher than antiaromatic singlet cyclobutadiene at the B3LYP/6-311G(d,p) level. Interestingly, for the square geometry of C_4H_4 MR-CCSD(T) calculations by Balkova and Bartlett[23] gave 6.9 kcal/mol for the energy difference between the ground singlet and the lowest triplet electronic states. Isomer **q2** can be described as a resonance of two electronic configurations:

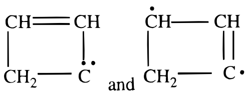

q2 is 22.1 kcal/mol less favorable than **q3** and has C_s symmetry with $^3A''$ electronic state. **q1** is a triplet analogue of singlet cyclobutyne studied by Schaefer and co-workers.[24] This isomer which also can be described as a triplet cyclobutyne lies 47.4 kcal/mol higher in energy than aromatic triplet cyclobutene **q3**. The energy difference can be attributed to the aromatic electron delocalization. The delocalization increases in the row **q1-q2-q3**, as does the relative stability. The bicyclic structure **q4** is similar to tetrahedrane, but with a CC bond broken giving two unpaired electrons. This isomer is 42.4 kcal/mol less favorable than the square structure **q3**. Interestingly, in the singlet electronic state the energy difference between antiaromatic cyclobutadiene and tetrahedrane is notably smaller, 26.0 kcal/mol at the G2 level of theory.[25] Thus, the planar four-membered ring structure is stabilized in the triplet state, and the nonplanar bicyclic structure is destabilized.

Isomerization Pathways. Possible isomerization pathways of triplet C_4H_4 are illustrated in Figure 2. The relative energies (in kcal/mol) with respect to C(^3P_j) + C_3H_4 (allene) of various isomers and transition states are shown in this figure in italic numbers. The energies of transition states are positioned near the lines connecting different local minima. Optimized geometries of transition states are drawn in Figure 3. The notation of TS's includes the names of the isomers connected by these transition states. For example, the transition state for the **c1** → **c3** isomerization is denoted as c1-c3. Figure 2 represents a graph describing the triplet PES of C_4H_4, and various routes from one local minimum to another can be found in this graph.

The rearrangements of C_4H_4 can be classified as hydrogen shifts and ring opening/closures related to three- and four-membered ring isomers. Chain structures can isomerize to each other by hydrogen migrations. For example, **c1** can eventually rearrange into **c5** by three consecutive H shifts via **c3** and **c4**. Typically, barriers for the hydrogen migrations are in the range of 40−60 kcal/mol. Transition state c1-c3 for the 1,2-H shift leading from **c1** to **c3** lies 61.7 and 40.6 kcal/mol higher than the former and the latter, respectively. Isomers **c3** and **c4** are connected by two transition states, c3-c4 and c3-c4′. The former corresponds to the 2,3-H shift and the latter to the 1,4-H shift in **c3** and lies about 6 kcal/mol higher in energy than c3-c4. The 1,4-H shift is also possible in **c1** directly yielding **c5**; however, the transition state c1-c5 has an unfavorable highly bent structure, and the barrier is very high, 88.6 kcal/mol relative to **c1**. In less stable chain isomers the hydrogen shift barriers can be low. For instance, **c6** is separated from **c5** by the barrier of only 0.2 kcal/mol. Thus, **c6** is kinetically unstable and should rapidly rearrange to **c5** by the 1,2-H shift to the terminal carbene-like carbon. As will be seen below, this fast isomerization can play an important role for the C(^3P_j) + C_3H_4 (propyne) reaction.

---

[22] (a) Bernardi, F.; Celani, P.; Olivucci, M. Robb, M. A., Suzzi-Valli, G. *J. Am. Chem. Soc.* **1995**, *117*, 10531. (b) Schleyer, P. v. R.; Maerker, C.; Dransfeld, A.; Jiao, H.; van Eikema Hommes, N. J. R. *J. Am. Chem. Soc.* **1996**, *118*, 6317.

[23] Balková, A.; Bartlett, R. J. *J. Chem. Phys.* **1994**, *101*, 8972.

[24] Carlson, H. A.; Quelch, G. E.; Schaefer, H. F., III. *J. Am. Chem. Soc.* **1992**, *114*, 5344.

[25] Glukhovtsev, M. N.; Laiter, S.; Pross, A. *J. Phys. Chem.* **1995**, *99*, 6828.

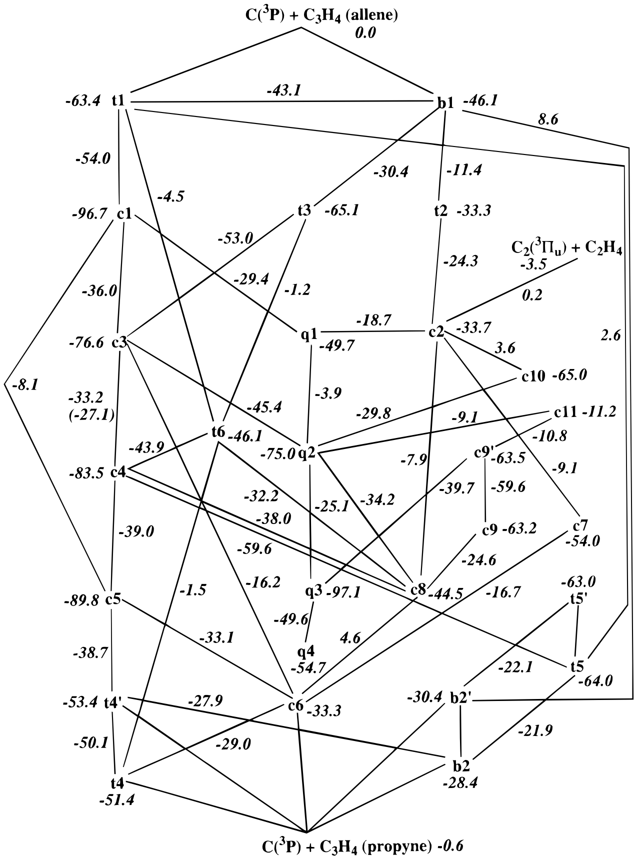

Figure 2. A graph of possible isomerization pathways on the global potential energy surface of triplet C_4H_4. Italic numbers show relative energies (in kcal/mol) for each isomer and transition state with respect to $C(^3P_j) + C_3H_4$ (allene), calculated at the G2M(RCC,MP2) level. The relative energy of $C_2(^3\Pi_u) + C_2H_4$ is given at the RCCSD(T)/6-311+G(3df,2p) + ZPE[B3LYP/6-311G(d,p)] level (see text for more detail).

The other routes connecting chain isomers include **c3** → **c6** → **c8** → **c9** → **c9′** → **c11**, **c6** → **c7** → **c2**, **c8** → **c2** → **c10**, and **c8** → **c4**. The latter corresponds to the vinylvinylidene → vinylacetylene rearrangement in triplet electronic state. The calculated barrier, 6.5 kcal/mol relative to **c8**, is somewhat higher than that for the similar process in the singlet state, 3.3 and 4.1 kcal/mol at the CISD/D95(d,p)[21] and G2M(rcc,MP2)[26] levels, respectively.

Branching isomers can undergo ring closure to form more stable three-membered ring structures with relatively low barriers. For example, the **b1** → **t1** and **b2** → **t4′** isomerizations have the barriers of 3.0 and 0.5 kcal/mol, respectively. In the **b1** → **t2** process leading to a less-stable three-membered ring isomer the barrier is higher, 34.7 kcal/mol. In some cases ring-closure is accompanied with a hydrogen migration, as for **b1** → **t3**, **b2** → **t5**, and **b2′** → **t5′**. The barriers for these reactions are in the range 6.5−15.7 kcal/mol. A simple hydrogen shift in the branching isomers is unlikely, since the barrier for **b1** → **b2′** is high, 54.7 kcal/mol relative to **b1**.

Three-membered ring structures can ring-open not only to the branching structures, but also to more stable chain isomers. **t1** and **t4′** give **c1** and **c5** by the ring-opening with the barriers of 9.4 and 14.7 kcal/mol, respectively. Similar processes in **t2**, **t3**, **t5**, and **t6** result in **c2**, **c3**, and **c4** with the barriers from 2.2 to 4.4 kcal/mol for **t6** and **t5** to 9−12 kcal/mol for **t2** and **t3**. If the ring-opening is endothermic, as for **t4** → **c6** and **t6** → **c8**, the corresponding barriers are higher, 21−22 kcal/mol. Hydrogen migrations which do not destroy the three-membered cycles in the "t"-isomers, **t1** → **t5**, **t1** → **t6**, **t3** → **t6**, and **t4** → **t6**, exhibit very large barriers of 50−65 kcal/mol. Hence, the three-membered ring isomers would rather rearrange to the chain structures than to each other.

Four-membered ring isomers can be formed from the chain structures by ring-closures: **c1** → **q1**, **c2** → **q1**, **c3** → **q2**, **c8** → **q2**, **c10** → **q2**, **c11** → **q2**, and **c9′** → **q3**. However, the barriers for such processes are usually high, except for relatively unstable isomers **c11**, **c2**, and **c8**. The reverse barriers characterize kinetic stability of the four-member ring structures. For instance, nonaromatic cyclobutene **q1** can isomerize to the very stable isomer **c1** with the barrier of 20.3 kcal/mol at the G2M(RCC,-MP2) level. The analogous process in the singlet state was calculated to have the classical barrier of 41.3 kcal/mol at the CCSD(T)/DZP level, but Schaefer and co-workers[24] gave the best estimate for the cyclobutyne → butatriene rearrangement barrier as ~25 kcal/mol. In any case, triplet cyclobutyne **q1** is expected to be less stable with respect to the ring opening than singlet cyclobutyne. On the other hand, aromatic triplet cyclobutene **q3** is much more stable; the ring opening barrier is 57.4 kcal/mol. Bicyclic structure **q4** is produced from **q3** with a barrier of 47.5 kcal/mol. The triplet tetrahedrane is not expected to be kinetically stable, since the reverse barrier for **q4** → **q3** is only 5.1 kcal/mol. 1,2-Hydrogen migrations connect **q1**, **q2**, and **q3**. The barrier heights for the H shifts range between 46 and 72 kcal/mol. Interestingly, the more favorable path for the rearrangement of **q1** to **q2** is not the direct H shift **q1** → **q2** but the multistep mechanism involving ring opening, hydrogen migration, and ring closure: **q1** → **c1** → **c3** → **q2**.

Dissociation Channels. Numerous hydrogen elimination routes shown in Figure 4 lead from chain and cyclic isomers of triplet C_4H_4 to various structures of the C_4H_3 radical (Figure 5). Normal C_4H_3 (n-C_4H_3, **p1**), the most stable isomer, can be produced from **c1**, **c3**, **c4**, and **c5**. Our calculations give the CH bond strength in **c1** as 53.7 kcal/mol. The reverse reactions n-C_4H_3 + H on the triplet PES are found to have barriers varying from 2.2 kcal/mol to produce **c1** to 6.0 kcal/mol to form **c3**. Transition states for hydrogen splitting shown in Figure 3 all have a late character (close to separated C_4H_3 + H) with the CH distances for the breaking bond between 1.9 and 2.3 Å. It is worth mentioning that singlet C_4H_4 can be formed from C_4H_3 + H without barrier. The geometry of n-C_4H_3 is of special interest. B3LYP/6-311G(d,p) optimization converges to a linear structure of C_{2v} symmetry which has no imaginary frequencies. However, earlier ab initio MO calculations at different levels of theory showed[27] that the linear C_{2v} structure actually is an inversion transition state and the minimum has a nonlinear geometry. Therefore, we reoptimized the structure of **p1** at the CCSD(T)/6-311G(d,p) level and confirmed that n-C_4H_3 is nonlinear and the linear geometry corresponds to the transition state. The energy difference between **p1** and linear TS is only 255 cm^{-1} at the CCSD(T)/6-311G(d,p) level with ZPE.

The second most stable isomer of C_4H_3 is i-C_4H_3, about 11 kcal/mol higher than **p1**. It can be produced in two conformations **p2** and **p2′** which are very close in energy. i-C_4H_3 is formed from **c3** and **c4** with low exit barriers of 1.4 and 2.7 kcal/mol and from less stable **c9** and **c10** with higher exit barriers (5−7 kcal/mol). In the energetical order, **p1** and **p2** are followed by cyclic structures of C_4H_3, **p3**, **p11**, and **p4** lying

---

[26] Mebel, A. M.; Chakraborty, D.; Park, J.; Lin, M. C.; Lin, S. H.; Lee, Y. T., to be published.

[27] (a) Ha, T.-K.; Gey, E. *J. Mol. Struct. (THEOCHEM)* **1994**, *306*, 197. (b) Cooksy, A. L. *J. Am. Chem. Soc.* **1995**, *117*, 1098. (c) Wang, H.; Cooksy, A. L. *Chem. Phys.* **1996**, *213*, 139.

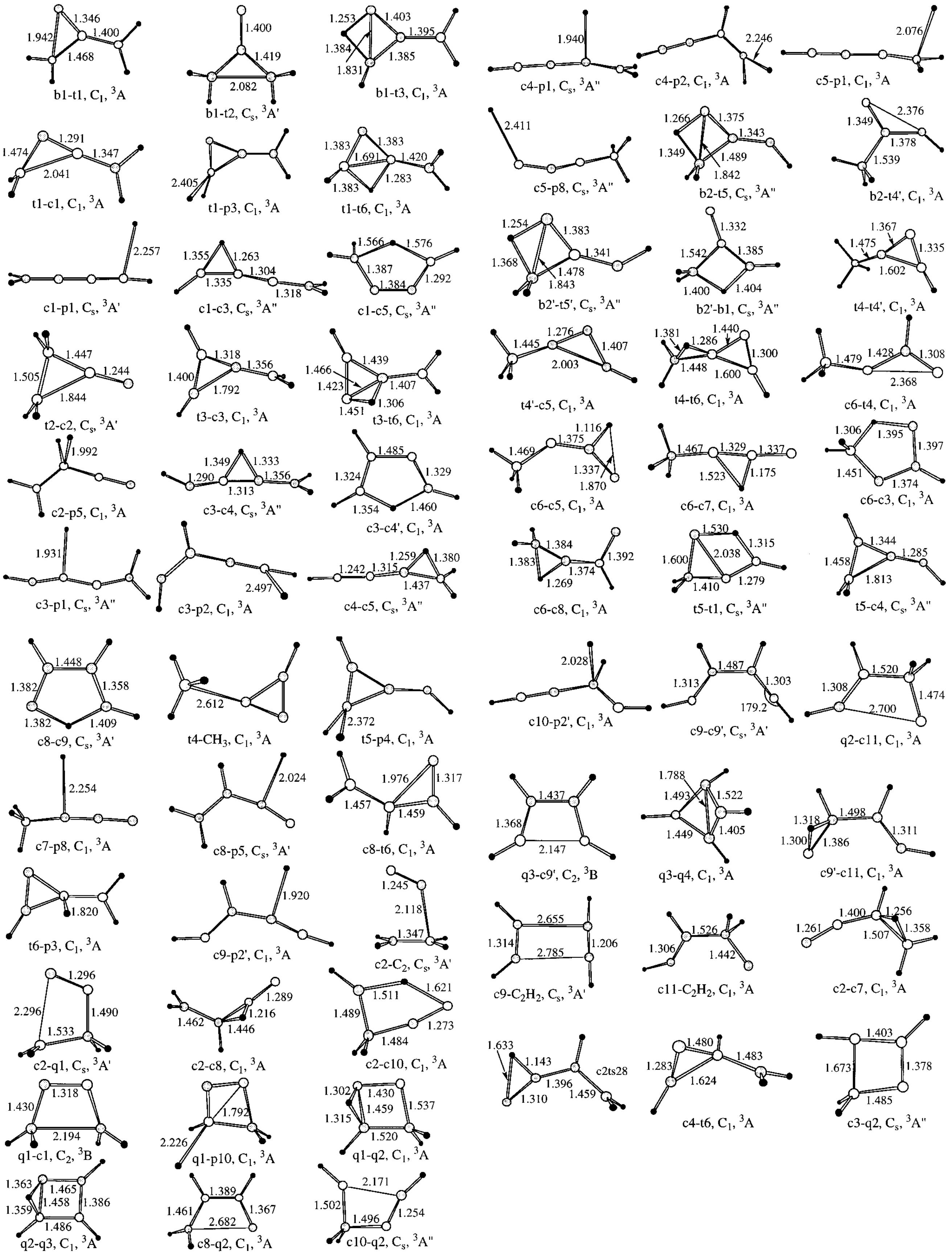

Figure 3. Optimized geometries of various transition states for triplet C_4H_4. (Selected bond lengths are shown in angstroms).

29.6, 31.3, and 31.8 kcal/mol higher than *n*-C_4H_3, respectively. Three-membered ring **p3** is produced from **t1** and **t6** with exit barriers of 1.4 and 9.7 kcal/mol and from **t3** and **t4** without exit barriers. **p4** which also has a three-membered ring structure can be formed from **t3** without reverse barrier and from **t5** with small exit barrier of 1.3 kcal/mol. Hydrogen elimination in **q2** leads to the four-membered ring C_4H_3 isomer **p11**, and no exit barrier was found.

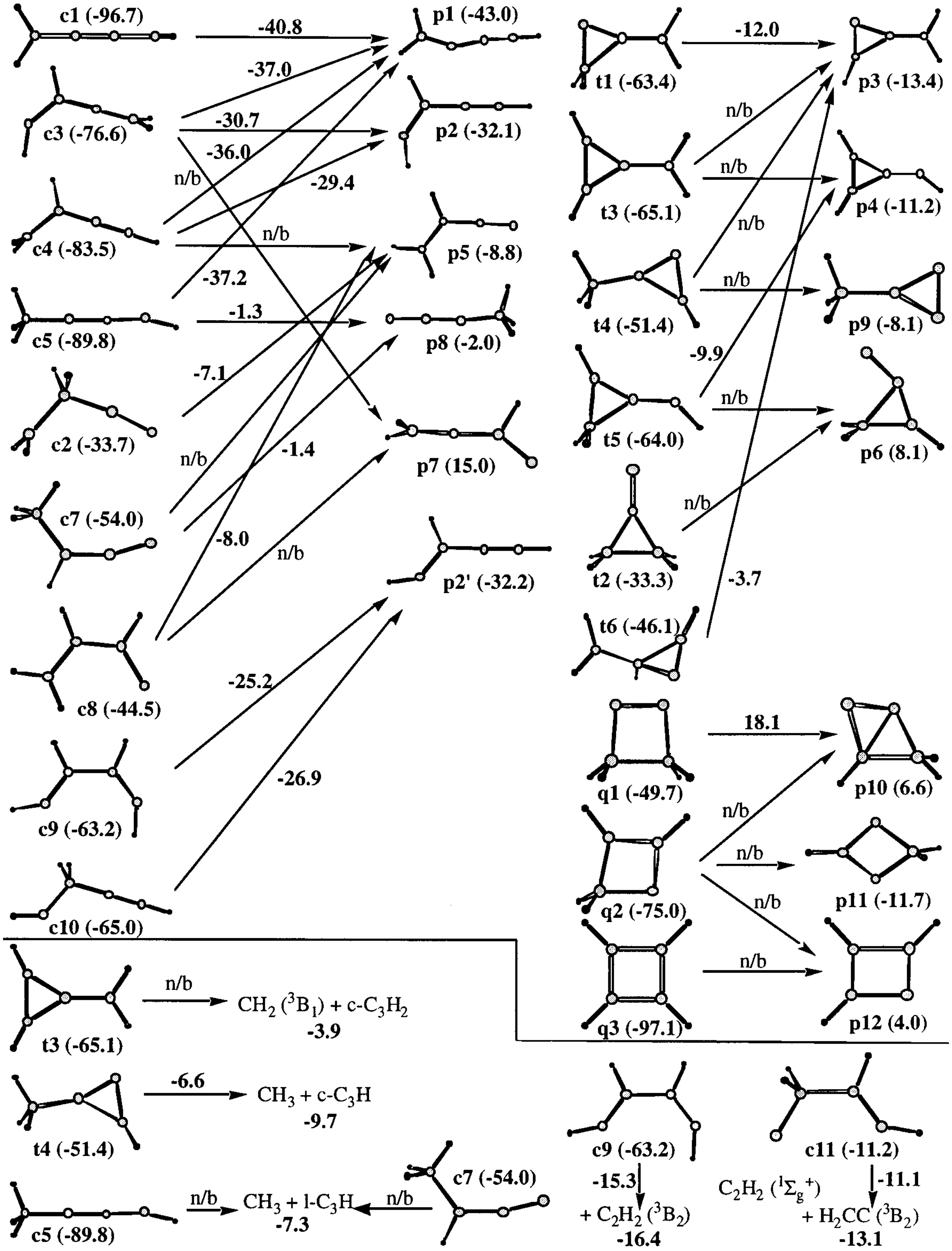

Figure 4. Various dissociation pathways for triplet C_4H_4. The numbers show relative energies (in kcal/mol) for each isomer and dissociation product with respect to C(^3P_j) + C_3H_4 (allene), calculated at the G2M(RCC,MP2) level. The numbers marking arrows correspond to the relative energies of dissociation transition states. The notation "n/b" means that a dissociation channel proceeds without an exit barrier.

Another chain isomer **p5** of the C_4H_3 radical, 34.2 kcal/mol above **p1**, can be obtained by hydrogen elimination from **c4** (no barrier), **c2** (exit barrier of 1.7 kcal/mol), **c7** (no barrier), and **c8** (0.8 kcal/mol barrier). Slightly less stable three-membered ring structure **p9** is formed from **t4** without barrier. The chain CH_3CCC structure **p8**, 41.0 kcal/mol less stable than *n*-C_4H_3, can react with H on the triplet PES yielding **c7** with a barrier of only 0.6 kcal/mol. The other C_4H_3 isomers, such as chain **p7**, three-membered ring **p6**, four-membered ring **p12**, and bicyclic **p10**, are 47−58 kcal/mol higher than **p1** and their production from triplet C_4H_4 is significantly endothermic and occurs without barrier. The **q1** → **p10** + H reaction is an exception; the reverse barrier reaches 11.7 kcal/mol. This can be attributed to that the hydrogen loss in **q1** is accompanied with the formation of extra CC bond and the structure changes from a four-membered ring to a bicycle. Indeed, the critical CC distance decreases from 2.10 Å in **q1** to 1.79 Å in TS q1-p10 and 1.59 Å in the product. Summarizing, we can say that

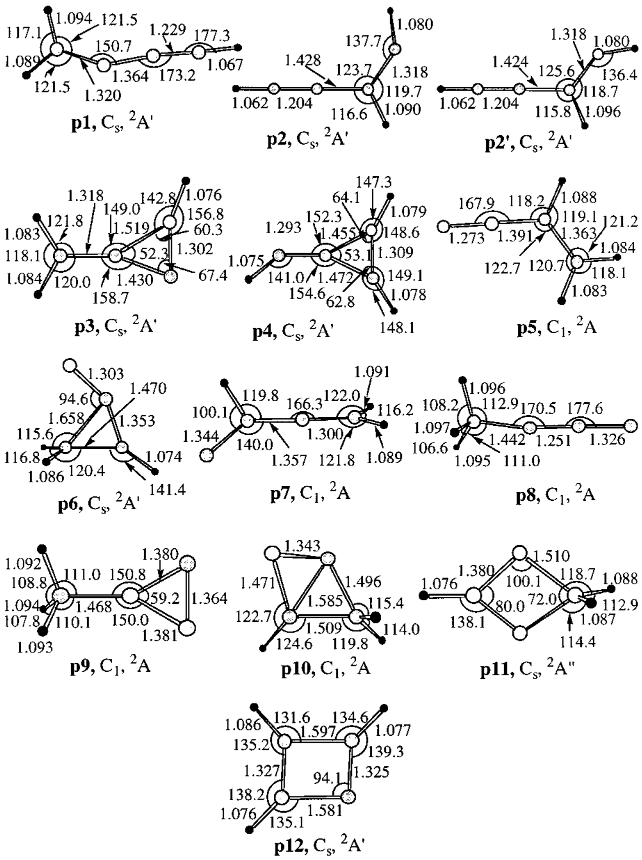

Figure 5. Optimized geometries (bond lengths are in angstroms, bond angles are in degrees) of various local minima for the C_4H_3 radical.

13 distinct isomers of the C_4H_3 radical can be produced from triplet C_4H_4. The hydrogen loss reactions are endothermic and take place with exit barriers from zero (no barrier) to ~10 kcal/mol.

Dissociation products other than C_4H_3 are also possible. Branching and some three-membered ring structures can lose a carbon atom giving $C(^3P_j)$ + C_3H_4 (allene and propyne) without exit barrier. **c2** can eliminate triplet C_2 producing ethylene. We will consider the reverse reactions in the subsequent sections. Dissociation of **t3** can result in CH_2 ($^3B_1$) + cyclo-C_3H_2 without barrier and with endothermicity of 61.2 kcal/mol. Methyl radical CH_3 can be emitted through the single CC bond cleavage in **t4** yielding cyclo-C_3H with exit barrier of 3.1 kcal/mol and from **c5** and **c7** without barrier. The CH_3 loss in **c5** and **c7** leads to the linear C_3H isomer. The structure **c9** can decompose to the singlet ($^1\Sigma_g{}^+$) and triplet ($^3B_2$) acetylenes. This reaction is endothermic by 46.8 kcal/mol and the reverse barrier is only 1.1 kcal/mol. Finally, the unstable isomer **c11** fragments to acetylene and triplet ($^3B_2$) vinylidene with a barrier of only 0.1 kcal/mol and the energy gain is 1.9 kcal/mol.

We should mention that the B3LYP approach is not always successful in finding dissociation transition states. For some channels we were not able to locate any TS at this level and the B3LYP TS optimization converged to the dissociation products. In this case, we tested the existence or nonexistence of TS's using MP2/6-311G(d,p) optimization. In most occasions the MP2 and B3LYP results agree. However, two transition states, c5-p8 and c2-C_2, were located only at the MP2 level.

PES of the $C(^3P_j)$ + H_2CCCH_2 Reaction. Now we are in position to apply our knowledge of the global C_4H_4 potential energy surface in triplet state to the reactions of our interest. First, we consider the reaction of carbon atom with allene which was recently studied by the crossed molecular-beam technique.[6] The profile of PES for this reaction is illustrated in Figure 6. We showed there only energetically preferable channels, other, less important reaction mechanisms can be found on the PES graph in Figure 2.

$C(^3P_j)$ can add without entrance barrier to one allenic C═C bond of H_2CCCH_2 to form the cyclic isomer **t1** which is stabilized by 63.4 kcal/mol with respect to the reactants. **t1** ring opens with a barrier of 9.4 kcal/mol to much more stable linear structure **c1** which is bound by 96.7 kcal/mol relative to $C(^3P_j)$ + allene. In addition, **t1** can lose a hydrogen atom yielding the C_4H_3 isomer **p3**. This product channel has the overall exothermicity of 13.4 kcal/mol and the exit barrier only 1.4 kcal/mol above **p3** + H. **c1** can emit a H atom to form the *n*-C_4H_3 isomer **p1** through a product like transition state located 2.2 kcal/mol above *n*-C_4H_3 + H. The reaction exothermicity for this channel is calculated as 43.0 kcal/mol. This amount is available for the translational and internal energy of the products in the molecular-beam experiment.[6] **c1** can also undergo a 1,2-H migration to form isomer **c3**. The barrier for this migration lies 36.0 kcal/mol below the reactants but 4.8 kcal/mol higher than the barrier for the hydrogen elimination. **c3** can fragment via CH bond cleavage to three different C_4H_3 isomers, **p1**, **p2**, and **p7**, but the pathway to **p7** is overall 15.0 kcal/mol endothermic. The formation of *i*-C_4H_3 **p2** + H from $C(^3P_j)$ + H_2CCCH_2 has the exothermicity of 32.1 kcal/mol. The exit barriers of the pathways leading from **c3** to **p1** and **p2** are 6.0 and 1.4 kcal/mol, respectively. Hydrogen migrations can continue in **c3** leading to **c4** and **c5**, which in turn can eliminate a hydrogen atom forming *n*- and *i*-C_4H_3 as well as some other isomers of this radical. However, our earlier RRKM calculations based on this PES demonstrated[6] that the isomerization of **c3** is unlikely in the conditions of the molecular-beam experiment and the *n*- and *i*-C_4H_3 products are almost exclusively formed from **c1** and **c3**.

In another reaction, channel $C(^3P_j)$ could attack the central carbon atom of the allene molecule without an entrance barrier to form the branching structure **b1**. The initial reaction step is less exothermic than the one leading to **t1**; the energy gain is 46.1 kcal/mol. The fate of **b1** can be 3-fold if we rule out an H migration to **b2′** because it has a very high barrier, 54.7 and 8.6 kcal/mol above **b1** and the reactants, respectively. First, the barrier to ring closure yielding **t1** is only 3.0 kcal/mol. After the **b1** → **t1** isomerization, this pathway merges with the channel described in the previous paragraph. Second, a H atom migration combined with a ring closure can form another three-membered ring isomer **t3** through the transition state b1-t3, 15.7 kcal/mol above **b1**. **t3** is stabilized by 65.1 kcal/mol with respect to the reactants. CH bond rupture in **t3** can yield either the C_4H_3 isomers **p3** or **p4**. The total reaction exothermicities of the **p3** and **p4** product channels are 13.4 and 11.2 kcal/mol, respectively. **t3** could also ring open through a barrier of 12.1 kcal/mol to **c3**. Additionally, **t3** might split the CH_2 group yielding CH_2 ($^3B_1$) and c-C_3H_2 without an exit barrier, but the reaction exothermicity is only 3.9 kcal/mol, making this channel unlikely. Third, **b1** might undergo a ring closure to form **t2** through a barrier of 34.7 kcal/mol. In principle, **t2** can show a barrierless CH bond rupture to produce the C_4H_3 isomer **p6**; however, this product channel is endothermic by 8.1 kcal/mol and unlikely to happen. The **t2** ring opens to isomer **c2** (the barrier is 9.6 kcal/mol) prior to CH bond rupture to form the C_4H_3 isomer **p5**. The channel leading from $C(^3P_j)$ + H_2CCCH_2 to C_4H_3 **p5** + H is exothermic by 8.8 kcal/mol and the the exit barrier is 1.7 kcal/mol. Also, **c2** could fragment to $C_2(^3\Pi_u)$ + C_2H_4, but

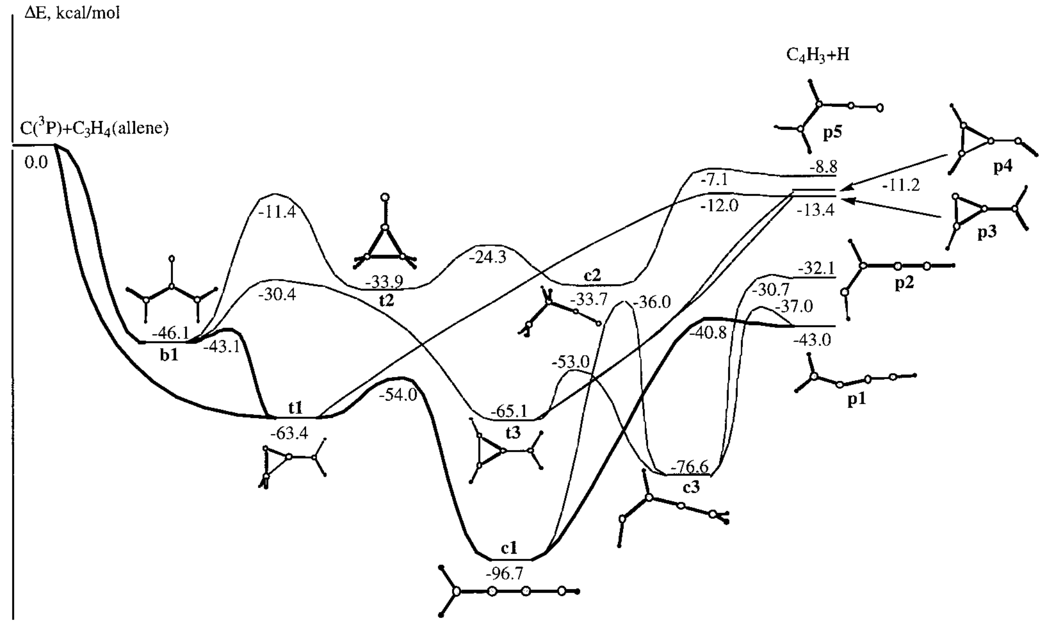

Figure 6. Profile of potential energy surface for the $C(^3P_j) + C_3H_4$ (allene) reaction calculated at the G2M(RCC,MP2) level.

this channel is energetically unfavorable as compared with the formation of **p5**. We shall address this pathway in detail in the section devoted to the $C_2(^3\Pi_u) + C_2H_4$ reaction. Finally, **c2** can isomerize to the four-member ring **q1** and then to the chain structure **c1** by consecutive ring closure and ring opening with the barriers of 15.0 and 20.3 kcal/mol, respectively. Transition states c2-q1 and q1-c1 lie 18.7 and 29.4 kcal/mol below the reactants.

Our calculations show that a direct insertion of the carbon atom into the allenic CH bond to form **c3** cannot occur. The latter can be produced only stepwise after the addition of $C(^3P_j)$ to the C=C bond or to the central C atom. We also considered earlier[6] the possibility of intersystem crossing (ISC) in the reaction leading the system onto the singlet C_4H_4 PES. ISC can occur in the vicinity of the isomer **b1** during its ring closure to **t1**. Singlet **t1** would isomerize to linear butatriene which emits a H atom to form n-C_4H_3 without exit barrier. However, the derived center-of-mass translational distribution $P(E_T)$ for the C_4H_3 product peaks at 7−12 kcal/mol indicating existence of a transition state for the decomposition of the C_4H_4 intermediate to the products. On this basis, we concluded earlier[6] that if ISC provides a reactive scattering signal of the $C(^3P_j) + H_2CCCH_2$ reaction, this contribution is likely small.

The RRKM calculations based on the PES described in this section showed that the major reaction product (more than 98.4%) should be n-C_4H_3 **p1**. The dominant portion of **p1**, 97−99%, is formed directly from the **c1** intermediate, and the rest comes from **c3**, with insignificant contributions from **c4** and **c5**. Therefore, the H migration from **c1** to **c5** plays a very minor role in the reaction. The second reaction product (less than 1.6% at the experimental collision energies of 4.7 and 9.3 kcal/mol) is i-C_4H_3 **p2** produced predominantly from **c3**. The results of theoretical calculations are in line with experimental observations in molecular beams.[6] For instance, the high energy cutoff of the $P(E_T)$ strongly suggest the formation of the n-C_4H_3 isomer **p1** and possibly i-C_4H_3 **p2**. The analysis of chemical dynamics for the $C(^3P_j) + H_2CCCH_2$ reaction showed that the carbon atom attacks the π-orbital of allene barrierless via a loose, reactant-like transition state located at the centrifugal barrier. The initially formed three-membered ring intermediate **t1** rotates in a plane almost perpendicular to the total angular momentum vector around its C-axis and undergoes ring opening to the chain intermediate **c1**. The latter decomposes via hydrogen atom emission to the n-C_4H_3 isomer. As the collision energy increases, the approach geometries with a small impact parameter very likely show an enhanced contribution leading possibly to a barrierless attack of $C(^3P_j)$ to the central carbon atom in H_2-$CCCH_2$ allene.

PES of the $C(^3P_j) + H_3CCCH$ Reaction. The calculated profile of PES for the reaction of carbon atom with methylacetylene (propyne) is illustrated in Figure 7 where we show only the channels preferable by energy. At the initial reaction step, five distinct isomers of triplet C_4H_4 can be formed without an entrance barrier. $C(^3P_j)$ can add to the acetylenic C≡C bond in H_3CCCH to yield cyclic isomers **t4** and **t4′** which are stabilized by 50.8 and 52.8 kcal/mol, respectively, relative to the reactants. **t4** would rapidly rearrange to **t4′** since the barrier separating them is only 1.3 kcal/mol. **t4′** ring opens with a barrier of 14.7 kcal/mol to the stable chain structure **c5**, H_3-CCCCH, which is bound by 89.2 kcal/mol with respect to $C(^3P_j)$ + propyne. In addition, **t4** and **t4′** can lose a hydrogen atom from two different positions (from the methyl group and from the ring CH) yielding the C_4H_3 isomers **p3** and **p9**. Both H eliminations occur without an exit barrier, and the calculated exothermicities for the C_4H_3 product channels are 12.8 kcal/mol for **p3** and 7.5 kcal/mol for **p9**. **c5** can emit an H atom from CH_3 to form the n-C_4H_3 isomer **p1** through the transition state c5-p1 located 5.8 kcal/mol above **p1** + H. The reaction exothermicity to produce n-C_4H_3 + H from $C(^3P_j) + H_3CCCH$ is 42.4 kcal/mol. Hydrogen emission from the CH group in **c5** would result in C_4H_3 **p8**. This channel is overall exothermic by 1.4 kcal/mol and has an exit barrier of 0.7 kcal/mol. Due to unfavorable energetics, the formation of **p8** is unlikely. **c5** can also show a 1,2-H shift to form isomer **c4**. The barrier for this rearrangement, 50.8 kcal/mol relative to **c5**, lies 38.4 and 1.8 kcal/mol below the reactants and the transition state for the H elimination to n-C_4H_3. In turn, **c4** can decompose via CH bond cleavage to three different isomers of C_4H_3, **p1**, **p2**, and **p5**. The **p1** channel is the most favorable; it has a reverse barrier of 7.0 kcal/mol. This is followed by the **p2** channel, 31.5 kcal/mol exothermic for the $C(^3P_j) + H_3CCCH$ reaction and with the exit barrier of 2.7 kcal/mol. The channel leading to **p5** is

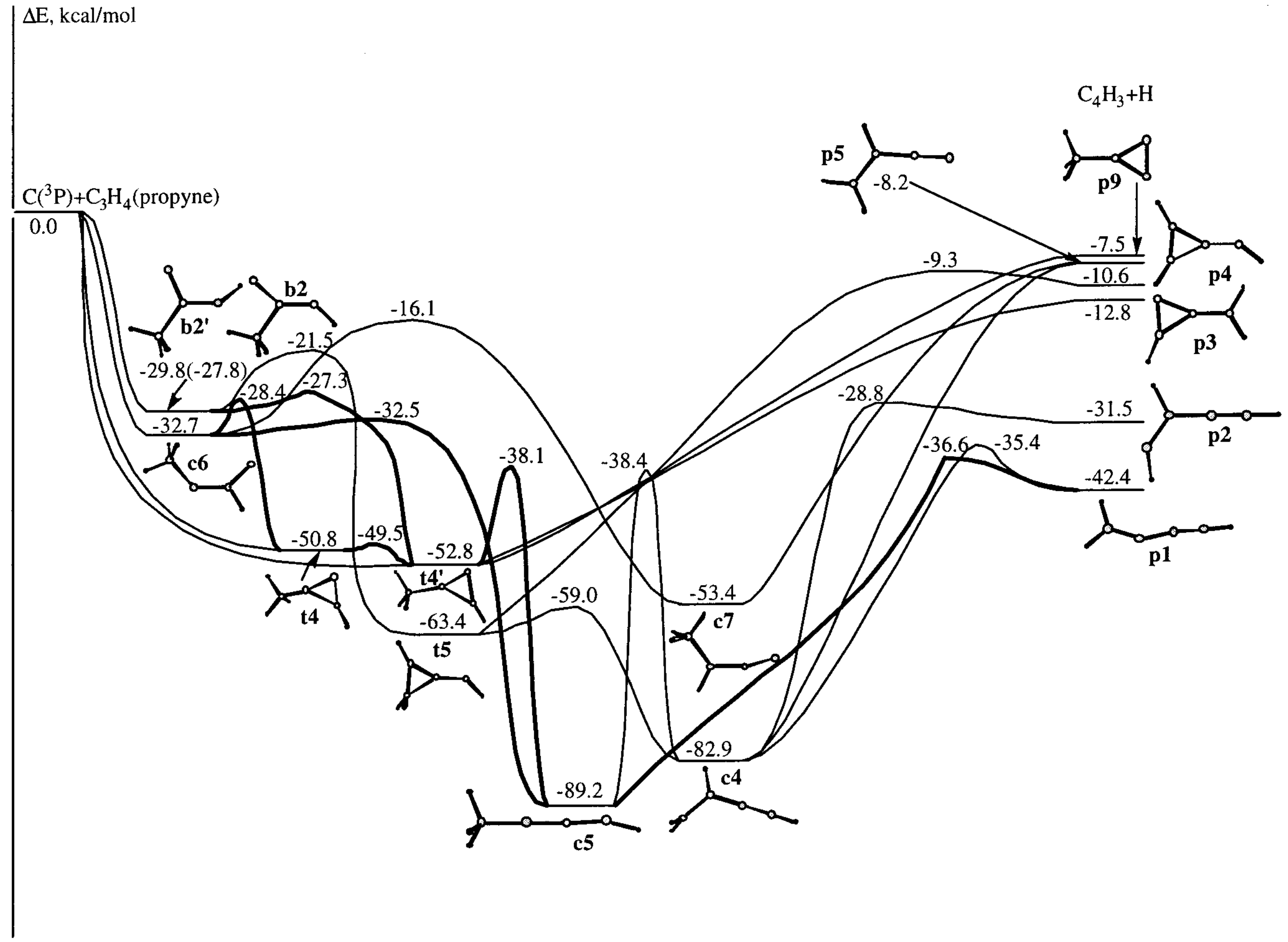

Figure 7. Profile of potential energy surface for the C(^3P_j) + C_3H_4 (propyne) reaction calculated at the G2M(RCC,MP2) level.

the least preferable but still exothermic by 8.2 kcal/mol with no exit barrier. Further isomerization of **c4** by the hydrogen scrambling to **c3** and **c1** is unlikely to play a significant role in the reaction, since the **c4** → **c3** barrier is higher than that for **c4** → **p1**. The pathways connecting **c4** with **t6**, **c8**, and **q2** may have lower barriers, but these structures would rather isomerize back to **c4** or **c3** than yield some different products. For instance, if **t6** is formed from **c4**, the reverse barrier back to **c4** is only 2.2 kcal/mol, while the barriers to produce **t1**, **t3**, **t4**, **c8**, or **p3** are significantly higher, 41.6, 44.9, 44.6, 13.9, and 42.4 kcal/mol, respectively. If **c8** is produced, the barrier to go back to **c4** is 6.5 kcal/mol and that to form **q2** is 10.3 kcal/mol. The other possibilities are less likely; the barriers for isomerization of **c8** to **t6**, **c9**, **c2**, and **c6** as well as for dissociation of **c8** to **p5** and **p7** are in the range of 19−60 kcal/mol. From **q2**, it is much easier to go to **c3** with a barrier of 29.6 kcal/mol than in any other direction.

In another initial reaction channel C(^3P_j) could attack the CH carbon atom of the propyne molecule to form the chain isomer **c6**, H_3CCCHC. In principle, two conformations of the C atoms are possible in H_3CCCHC, cis, like in **c6**, and trans. However, the attempts to optimize the trans structure both at the B3LYP and MP2 levels resulted in **t4**, indicating that the trans conformation does not exist. It is worth mentioning that the cis conformation **c6** also collapsed to **t4** at the B3LYP level but MP2 optimization gives a local minimum. Therefore, the transition state c6-t4 was also computed at MP2/6-311G(d,p). **c6** is stabilized by 32.7 kcal/mol relative to the reactants but is very unstable kinetically. The barrier for the H shift from CH to the terminal carbon atom to yield **c5** is as low as 0.2 kcal/mol. **c6** also can easily show ring closure to give **t4** with a barrier of 4.3 kcal/mol. Other hydrogen migrations in **c6**, i.e., **c6** → **c7**, **c6** → **c3**, and **c6** → **c8**, require significantly higher barriers. In Figure 7, we showed only one of these channels, with the lowest barrier of 16.6 kcal/mol. It leads to the H_3CCCHCC isomer **c7**, 53.4 kcal/mol below the reactants. Methyl hydrogen splitting from **c7** gives the C_4H_3 isomer **p5** without exit barrier. Emission of the CH hydrogen which takes place with an exit barrier of 0.6 kcal/mol is unfavorable since it yields the C_4H_3 isomer **p8**, only 1.4 kcal/mol below the reactants. Further hydrogen migration in **c7** to **c2** is unlikely because of a high barrier.

Addition of C(^3P_j) to the carbon atom connected to CH_3 gives trans and cis branching structures **b2′** and **b2**, 29.8 and 27.8 kcal/mol below the reactants, respectively. **b2** undergoes ring closure to **t4′** with a barrier of only 0.5 kcal/mol. On the other hand, a ring closure accompanied with a hydrogen migration leads **b2** and **b2′** to the three-membered ring isomers **t5** and **t5′** with barriers of 6.5 and 8.3 kcal/mol, respectively. **t5** and **t5′** are stabilized by 63.4 and 62.4 kcal/mol with respect to the reactants. On the next step **t5** show ring opening to yield **c4** with a low barrier of 4.4 kcal/mol. Hydrogen emission from the CH_2 group in **t5** and **t5′** gives the C_4H_3 isomer **p4**, and the exit barrier for this process is calculated as 1.3 kcal/mol. The overall exothermicity of the **p4** + H product channel is 10.6 kcal/mol. The rupture of the out-of-ring CH bond in **t5** and **t5′** occurring without exit barrier is less likely, since the C_4H_3 + H product lie 8.7 kcal/mol above the reactants. Also, a 1,3-H shift connecting **t5** with **t1** is not feasible because of a very high barrier.

$CH_3 + C_3H$ products can be formed by the single CC bond cleavage in **t4**, **c5**, and **c7**. In the case of **t4**, cyclic C_3H is formed with an exit barrier of 3.1 kcal/mol and the exothermicity of the $C(^3P_j) + H_3CCCH \rightarrow CH_3 + c\text{-}C_3H$ reaction is calculated to be 9.1 kcal/mol. For **c5** and **c7**, the emission of CH_3 occurs without an exit barrier, and the total exothermicity for the $CH_3 + l\text{-}C_3H$ channel is 6.7 kcal/mol. Due to unfavorable energetics, the formation of $CH_3 + C_3H$ would play at best a minor role in the reaction of $C(^3P_j)$ with propyne. Similarly to the reaction with allene, a direct insertion of the carbon atom into the acetylenic or methyl CH bonds does not occur; the corresponding transition states could not be found. On the other hand, the insertion into the acetylenic bond is nearly direct: $C(^3P_j) + H_3CCCH \rightarrow$ **c6** $\rightarrow$ **c5**, where the addition intermediate is metastable and separated from **c5** by a tiny barrier. The insertion into a methyl CH bond of propyne would give **c10**. Instead, **c10** can be formed by multistep pathways where most of transition states lie below the reactants: ... $\rightarrow$ **c5** $\rightarrow$ **c4** $\rightarrow$ **c3** $\rightarrow$ **q2** $\rightarrow$ **c10** and ... $\rightarrow$ **c6** $\rightarrow$ **c7** or **c8** $\rightarrow$ **c10**. Finally, note that no C_4H_4 intermediates relevant for this reaction fulfills requirements for intersystem crossing,[5,7c] so we do not consider the singlet PES here.

From the experimental study of the $C(^3P_j) + H_3CCCH$ reaction in crossed molecular beams,[5] a conclusion was made that the reaction proceeds by the carbon atom attack to the π-orbitals of methylacetylene via a loose reactant like transition state at the centrifugal barrier with initial formation of triplet 1-methylpropendiylidene complex **c6**. **c6** rotates in a plane almost perpendicular to the total angular momentum vector around the B/C axes and undergoes a H migration to triplet 1-methylpropargylene **c5**. Within 1−2 ps, the latter decomposes via CH-bond cleavage to $n\text{-}C_4H_3$. The initial intermediates **b2**, **b2′**, **t4**, and **t4′** were considered less likely because of uneven spin density distribution on two triply bound carbons and the sterical hindrance of the CH_3 group which reduces the cone of acceptance at the α-C-atom and the range of reactive impact parameters. For instance, a simultaneous attack of $C(^3P_j)$ to α- and β-C-atoms to produce **t4** or **t4′** would give maximum impact parameter of 0.6 Å, while only narrow range of impact parameters between 1.19 and 2.24 Å actually contributes to the reactive scattering signal. From the PES presented here, it is difficult to judge what are relative initial concentrations of the **b2**, **b2′**, **c6**, **t4**, and **t4′** intermediates in the reaction, since all of them are formed exothermically without entrance barrier. Further studies including variational RRKM are needed to address this question.

At higher collision energies for both C_3H_4 isomers, crossed molecular beam data show almost identical data, indicating the two reactions produce similar products, major $n\text{-}C_4H_3$ and minor $i\text{-}C_4H_3$. The result is in line with the reaction PES which shows that the formation of $n\text{-}C_4H_3$ through intermediate **c5** is most favorable energetically and $i\text{-}C_4H_3$ can be reached via intermediate **c4**. At lower collision energies, the center of mass distributions differ significantly,[5] indicating that the reactions of carbon atom with propyne and allene form distinct isomers. On the basis of the high energy cutoff of the center of mass translational energy distribution, the authors suggested the formation of a higher energy isomer, possibly a cyclic one. On the basis of the present calculations, we can suggest that this isomer could be **p3** which can be produced from **t4′** without exit barrier. Formation of **p4** is much less likely because it has to go through the **t5** intermediate formed from **b2**. However, **b2** would rather isomerize to **t4′** than to **t5**. In the reaction with allene (Figure 6) the **p3** product can be generated from **t1**. The ring-opening barrier in **t1** is 5.3 kcal/mol lower than the corresponding barrier for **t4′**. Therefore, the lifetime of **t4′** should be longer than that of **t1**, so the former might have enough time to emit a hydrogen atom. To quantify our consideration of the product branching ratios in the $C(^3P_j) + H_3CCCH$ reaction, detailed RRKM calculations are now underway for different collision energies and with variation of initial concentrations of the **b2**, **b2′**, **c6**, **t4**, and **t4′** intermediates.

PES of the $C_2(^3\Pi_u) + C_2H_4$ Reaction. First, we look into the question what is the relative energy of $C_2(^3\Pi_u) + C_2H_4$ with respect to $C(^3P_j) + H_2CCCH_2$ which was chosen as zero on the PES map shown in Figure 2. From experimental heats of formation,[28] the $C(^3P_j) + H_2CCCH_2 \rightarrow C_2(^1\Sigma_g^+) + C_2H_4$ reaction is exothermic by 2.9 kcal/mol. Experimentally,[29] the $^3\Pi_u$ state of C_2 lies 2 kcal/mol higher in energy than $^1\Sigma_g^+$, so the $C(^3P_j) + H_2CCCH_2 \rightarrow C_2(^3\Pi_u) + C_2H_4$ reaction exothermicity is 0.9 kcal/mol. At the G2M(RCC,MP2) level, we found that the reaction leading to the singlet C_2 is exothermic by 9.8 kcal/mol, while that leading to the triplet C_2 is endothermic by 1.3 kcal/mol. Thus, in this approximation the energy gap between C_2 $^1\Sigma_g^+$ and $^3\Pi_u$ is greatly overestimated. G2M(RCC,MP2) includes RCCSD(T)/6-311G(d,p), MP2/6-311G(d,p), and MP2/6-311+G(3df,2p) calculations in order to estimate the RCCSD(T)/6-311+G(3df,2p) energy. The energy difference between $^1\Sigma_g^+$ and $^3\Pi_u$ is computed as 2.4 kcal/mol at RCCSD(T)/6-311G(d,p), and 0.8 and 6.5 kcal/mol at MP2 with smaller and larger basis sets, respectively. Thus, the MP2 method performs unsuccessfully for C_2, which could be foreseen taking into account a multireference character of the wave function in the carbon dimer. The singlet−triplet energy gap in C_2 at G2M(RCC,MP2) is further exaggerated due to the HLC correction.[13,14] The $^1\Sigma_g^+$ state formally has an extra electron pair as compared to $^3\Pi_u$, so the HLC correction[13] adds 3 kcal/mol into the stabilization of singlet C_2. On the other hand, the coupled cluster method provides satisfactory results; the RCCSD(T)/6-311+G(3df,2p) calculated $^1\Sigma_g^+$-$^3\Pi_u$ energy gap in C_2 is 1.8 kcal/mol. Therefore, we used this level to compute the energy difference between $C(^3P_j)$ + allene and $C_2H_4 + C_2$ in singlet and triplet states. The results, 5.3 and 3.5 kcal/mol for C_2 $^1\Sigma_g^+$ and $^3\Pi_u$, respectively, overestimate the experimental exothermicities by ∼2.5 kcal/mol, which is close to the accuracy usually expected for the heats of reactions from the G2-type methods. Hence, we use for $C_2(^3\Pi_u) + C_2H_4$ the RCCSD(T)/6-311+G(3df,2p) relative energy in comparison with G2M(RCC,MP2) relative energies for the other species on the triplet C_4H_4 PES. The comparison is warranted since G2M(RCC,MP2) approximates the RCCSD(T)/6-311+G(3df,2p) energy, but the correction scheme fails for C_2. Mention also that the HLC correction is not present in relative energies because all species on the PES have the triplet multiplicity.

Now we turn to the PES of the $C_2(^3\Pi_u) + C_2H_4$ reaction shown in Figure 8. In principle, a C_2 molecule can add to a C atom of ethylene yielding the triplet C_4H_4 isomer **c2** or to the CC π-bond in a perpendicular or parallel manner producing three-membered ring **t2** and four-membered ring **q1**, respectively. Addition to the carbon atom occurs with an entrance barrier at the transition state c2-C_2 ($^3A'$,C_s). This is an early TS with forming CC bond distance of 2.12 Å. C_2 is located in the plane perpendicular to the C_2H_4 plane, so the carbon dimer attacks the π-system of ethylene. The entrance barrier height is calculated to be 4.6 and 3.7 kcal/mol at the RCCSD(T)/6-311G-

---

(28) The experimental heats of formation are taken from *NIST Chemistry Webbook*; NIST Standard Reference DataBase Number 69, November 1998 Release (http://webbook.nist.gov/chemistry/).

(29) Martin, M. *J. Photochem. Photobiol. A: Chem.* **1992**, *66*, 263.

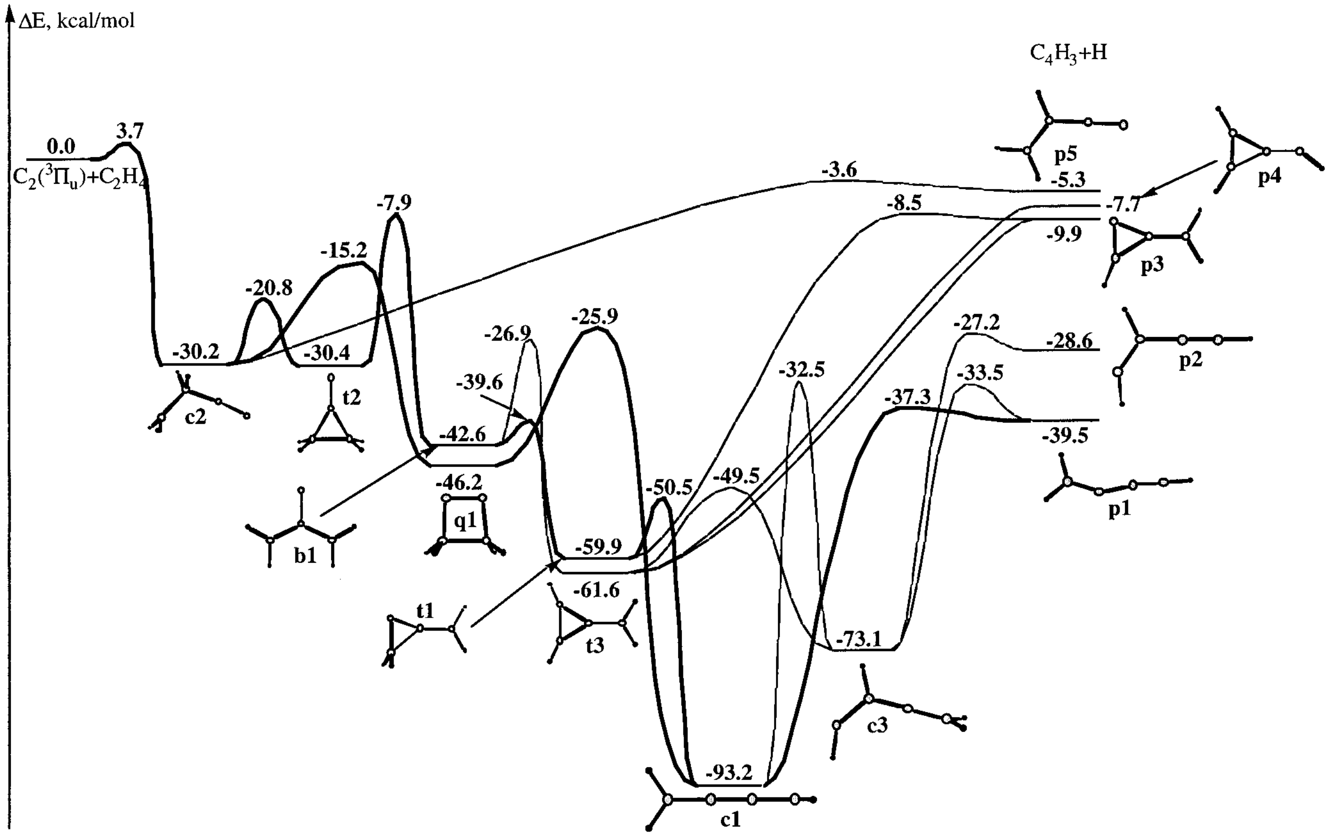

Figure 8. Profile of potential energy surface for the $C_2(^3\Pi_u) + C_2H_4$ reaction calculated at the G2M(RCC,MP2) level.

(d,p) and G2M(RCC,MP2)-RCCSD(T)/6-311+G(3df,2p) levels, respectively, including ZPE. Connection of the c2-C_2 TS with the **c2** local minimum was confirmed by the intrinsic reaction coordinate (IRC) calculations at the MP2/6-311G(d,p) level.

The parallel addition of $C_2(^3\Pi_u)$ to the π-bond of ethylene within C_{2v} geometry is symmetry-forbidden. In this case, the two components of the $C_2(^3\Pi_u)$ state split into $^3A_1$ and $^3B_1$ states for $C_2 + C_2H_4$ at infinite separation, while the electronic state of C_4H_4 **q1** is $^3B_2$. The perpendicular approach can be formally symmetry-allowed; the $^3\Pi_u$ state of C_2 splits into the $^3B_2$ and $^3B_1$ components for $C_2 + C_2H_4$ and the electronic state of the product **t2** is $^3B_2$. However, the electronic configurations for the two $^3B_2$ states are different: $8a_1^2 9a_1^1 2b_2^2 3b_2^1$ for $C_2(^3\Pi_u) + C_2H_4$ and $7a_1^2 8a_1^1 3b_2^2 4b_2^1$ for **t2**, so an electron pair has to be moved from the a_1 orbital to b_2. Therefore, **q1** and **t2** can be formed from the reactants either via a seam of crossing or avoided crossing (for the perpendicular approach) of two different electronic states or via nonsymmetric transition states. We located two minima on the seams of crossing, MSX1 and MSX2, shown in Figure 9. MSX1 corresponds to the perpendicular approach where the avoided crossing of two $^3B_2$ states with different electronic configurations takes place. MSX2 is related to the parallel approach and is a minimum on the $^3A_1$-$^3B_2$ seam of crossing. We took the $^3A_1$ component of the $^3\Pi_u$ state of C_2 because it is lower in energy than the $^3B_1$ component at finite separations between C_2 and C_2H_4. The calculations were carried out at the B3LYP/6-311G(d,p) level using the SEAM program.[30] At this level, MSX1 and MSX2, respectively, lie 31.7 and 14.1 kcal/mol higher than the reactants $C_2(^3\Pi_u) + C_2H_4$. The result indicates that the direct formation of **t2** or **q1** from the reactants with C_{2v} symmetry cannot compete with the formation of **c2** where the entrance barrier is only ~4 kcal/mol. When we tried to search for nonsymmetric transition states leading from the reactants to **t2** or **q1**, the optimization converged to TS c2-C_2 connecting $C_2(^3\Pi_u) + C_2H_4$ with the isomer **c2**. Thus, the three- and four-membered ring addition complexes are most likely to be formed indirectly, via the chain structure **c2**.

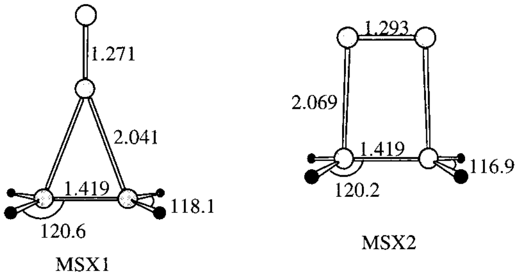

MSX1 MSX2

Figure 9. Optimized geometries of the minima on the seams of crossing of two triplet electronic states corresponding to the perpendicular and parallel approach of $C_2(^3\Pi_u)$ toward C_2H_4 within C_{2v} symmetry.

Besides emitting a H atom to yield the C_4H_3 isomer **p5** (5.3 kcal/mol below the reactants), there are two major pathways for **c2** isomerization. First, **c2** can show ring closure to **t2**, which in turn would rearrange to **b1** and then **t1**, and **c1**. This path was described in detail when we addressed PES for the $C(^3P_j) + H_2CCCH_2$ reaction. **c1** loses a hydrogen atom to produce *n*-C_4H_3 **p1** with overall exothermicity of 39.5 kcal/mol. The highest barrier on this pathway is located at TS b1-t2, 22.5 kcal/mol above **t2** but 7.9 kcal/mol below the reactants. The second route from **c2** to **c1** involves the four-member ring isomer **q1**. The ring closure from **c2** to **q1** requires a barrier of 15.0 kcal/mol, and the corresponding transition state is 15.2 kcal/mol lower in energy than the reactants. Then, **q1** undergoes ring

---

(30) (a) Cui, Q. Ph.D. Thesis, Emory University, 1997. (b) Dunn, K.; Morokuma, K. *J. Chem. Phys.* **1995**, *102*, 4904.

opening along the CH_2-CH_2 bond to yield **c1** with a barrier of 20.3 kcal/mol. The two pathways leading from **c2** to **c1** are expected to compete, and further RRKM calculations are required to quantify their roles in the $C_2(^3\Pi_u) + C_2H_4$ reaction. The other channels of rearrangement of **c2** by hydrogen migrations to **c7**, **c8**, or **c10** have significantly higher barriers than the ring closure and are not expected to play any important role.

From PES shown in Figure 8, we can conclude that for the $C_2(^3\Pi_u) + C_2H_4$ reaction, similarly to $C(^3P_j)$ + allene, n-C_4H_3 + H should be the major product, with possible minor production of i-C_4H_3 via the **c1** → **c3** → **p2** channel. Other isomers of C_4H_3 which might be produced are **p3**, **p4**, and **p5**, but their contribution is not expected to be significant. Of other products, in principle, acetylene could be formed in pair with triplet vinylidene H_2CC ($^3B_2$): **q1** → **c1** → **c3** → **q2** → **c11** → $C_2H_2 + H_2CC$ ($^3B_2$), or with triplet acetylene $^3B_2$: **q2** → **q3** → **c9′** → $C_2H_2 + C_2H_2$ ($^3B_2$) or **c2** → **c8** → **c9** → $C_2H_2 + C_2H_2$ ($^3B_2$). Although the two acetylene channels in the $C_2(^3\Pi_u) + C_2H_4$ reaction are exothermic by 9.6 and 12.9 kcal/mol, we do not expect them to compete with the channels yielding n- and i-C_4H_3 because of unfavorable energetic barriers. Detailed RRKM calculations are now underway to predict product branching ratios at various collision energies.

Recent molecular-beam experiments for the $C_2 + C_2H_4$ reaction[8] show n-C_4H_3 as the dominant product, and the experimental TOF spectra could be fitted in terms of contributions from two reactions $C_2(^1\Sigma_g^+) + C_2H_4$ and $C_2(^3\Pi_u) + C_2H_4$. We shall address the experimental data, the results of RRKM calculations for the triplet PES, and the singlet potential energy surface elsewhere.[8]

Conclusions

We have studied the global potential energy surface of C_4H_4 in the lowest triplet electronic state. Twenty eight distinct isomers are located as well as 66 transition states for various isomerization and dissociation pathways. The most stable structures for triplet C_4H_4 are aromatic cyclobutene **q3** ($^3A_{1g}$,D_{4h}) and linear butyne **c1** (^3E,D_{2d}) lying 0.4 kcal/mol higher in energy than **q3**. Other local minima include chains, branching configurations, three- and four-membered rings, and a bicyclic structure. Isomerization mechanisms in triplet C_4H_4 involve hydrogen migrations and ring opening/closures. At triplet PES, C_4H_4 can dissociate to $C(^3P_j) + C_3H_4$, $C_2(^3\Pi_u) + C_2H_4$, C_4H_3 (thirteen different isomers) + H, CH_2 ($^3B_1$) + c−C_3H_2, CH_3 + l/c−C_3H, and C_2H_2 ($^1\Sigma_g^+$) + C_2H_2 ($^3B_2$)/H_2CC ($^3B_2$).

The information about the global PES is applied to describe the potential energy surfaces for the $C(^3P_j) + H_2CCCH_2$, $C(^3P_j) + H_3CCCH$, and $C_2(^3\Pi_u) + C_2H_4$ reactions, recently studied in crossed molecular-beam experiments.[5,6,8] The reaction of the carbon atom with allene is shown to occur by the addition of C to the allenic C=C bond to yield the three-membered ring structure **t1** or (in a less extent) to the central carbon atom of allene to form the branching structure **b1** which isomerizes to **t1** with a low barrier. **t1** undergoes ring opening to **c1**, and the latter emits a H atom to give n-C_4H_3, the major reaction product. The minor reaction product, i-C_4H_3, is formed through a 1,2-H shift in **c1** leading to **c3** followed by the hydrogen loss.

The reaction of the carbon atom with methylacetylene starts with the C addition to the β-C-atom of H_3CCCH to form **c6**, to the α-C-atom to give **b2** or **b2′**, or to the acetylenic C≡C bond to yield the cyclic isomers **t4** or **t4′**. According to experimental impact parameters,[5] the formation of **c6** at the initial reaction step is most probable. **c6** is metastable and would rearrange to the linear isomer **c5** or to the cyclic **t4** and then to **t4′** with low barriers. **b2** and **b2′** should also rapidly isomerize to **t4′**. The latter ring opens to **c5** with the barrier of 14.7 kcal/mol. The major reaction product n-C_4H_3 is formed through the methyl hydrogen emission in **c5**. The second product i-C_4H_3 can be reached via a H-shift from **c5** to **c4** and subsequent hydrogen elimination. Cyclic isomers C_4H_3 **p3** and **p4** (formation of those was postulated from the experimental crossed molecular-beam measurements[5]) can originate from **t4**, **t4′**, and **t5**. Further RRKM calculations are required to quantify the product branching ratios in the reaction of $C(^3P_j)$ with propyne.

The reaction of $C_2(^3\Pi_u)$ with ethylene proceeds through the C_2 addition to a carbon atom of C_2H_4 to yield the chain isomer **c2** with an entrance barrier of ∼4 kcal/mol. **c2** rearranges to linear **c1** in two steps via the four-membered ring intermediate **q1**: **c2** → **q1** → **c1**, or by a multistep mechanism involving three-member ring structures: **c2** → **t2** → **b1** → **t1** → **c1**. **c1** loses an H atom to yield n-C_4H_3 or undergoes a hydrogen migration to **c3** followed by a H emission producing n- or i-C_4H_3. Similarly to the $C(^3P_j)$ + allene reaction, n-C_4H_3 is expected to be the major product of $C_2(^3\Pi_u) + C_2H_4$, while i-C_4H_3 to give a minor contribution.

Acknowledgment. This work supported by Academia Sinica and in part by the National Science Council of ROC under Grant NSC 8902113-M-001-034. A partial support from the Petroleum Research Fund of the Republic of China is also appreciated. The authors thank the reviewers for their valuable corrections.

JA9935299